

# Opening carbon nanotubes into zigzag graphene nanoribbons by energy-optimum oxidation

Yufeng Guo,<sup>\*</sup> Lai Jiang, and Wanlin Guo<sup>†</sup>*Institute of Nanoscience, Nanjing University of Aeronautics and Astronautics, Nanjing 210016, China*

(Received 19 May 2010; revised manuscript received 17 August 2010; published 21 September 2010)

Narrow zigzag graphene nanoribbons are found to have exceptional electronic and magnetic properties but difficult to fabricate. We show by density-functional calculations and an elastic mechanical model that oxygen atoms have strong energetic favorability to adsorb on small-diameter carbon nanotubes and form unzipped C-O-C epoxy chains along a direction of minimum angle to the tube axis. With other oxygen atoms further attacking, the unzipping epoxy chain formed on the energy-optimum direction of the nanotube is broken into carbonyl pairs. These results promise that unique zigzag graphene nanoribbons could be fabricated by oxidation of small-diameter carbon nanotubes with arbitrary chiralities according to the minimum energy principle.

DOI: 10.1103/PhysRevB.82.115440

PACS number(s): 61.46.Fg, 61.48.Gh, 68.35.Gy, 68.47.Gh

## I. INTRODUCTION

Graphene nanoribbon (GNR), one-dimensional (1D) strip of single carbon layer with a width in nanometer scale, possesses specific edge states and attracts numerous scientific interests for its potential applications in nanodevices and spinelectronics.<sup>1-5</sup> In particular, zigzag GNRs with widths less than 10 nm are found to have exceptional electronic and magnetic properties,<sup>6-10</sup> and zigzag nanoribbons on silicon substrates can exhibit intriguing magnetoelectric effects.<sup>11</sup> Nevertheless, to fabricate such narrow GNRs with desired sizes and smooth edges remains a challenge. Carbon nanotubes as an allotrope of GNRs now can be synthesized with controllable diameter. Recent experiments reported that GNRs can be fabricated from longitudinally breaking carbon nanotubes by plasma etching,<sup>12</sup> lithium intercalation and exfoliation,<sup>13</sup> and chemical oxidation.<sup>14,15</sup> The edge geometry of the obtained nanoribbons by these methods may depend on the chiralities of mother carbon nanotubes, which, however, are still uncontrollable.

Oxidation is an important way to tune and manipulate the structural and physical properties of carbon nanomaterials.<sup>16-20</sup> The atomistic mechanisms of oxidation-induced unzipping of graphite sheets and carbon nanotubes<sup>21</sup> as well as oxidatively breaking carbon nanotubes into GNRs (Ref. 22) have been theoretically studied. Another work reported that flat graphene can be oxidatively cut with formation of smooth zigzag edges.<sup>23</sup> However, it is still not clear which site in the hexagonal lattices of carbon nanotubes or graphene sheets and subsequent oxygen adsorption direction are more favorable from the oxidation beginning. For oxidative fabrication of GNRs from carbon nanotubes, the oxidation direction along the nanotubes should be the most important determinant to control the size and edge structure of the obtained GNRs.

In this study, using first-principles calculations and an elastic mechanics model we show that there is an energy-optimum direction for O atoms to adsorb and subsequently form unzipped C-O-C epoxy chain on single-walled carbon nanotubes (SWNTs) of small diameters. By further oxidizing the formed unzipped epoxy chains, small-diameter SWNTs

with arbitrary chiralities could be opened into narrow GNRs with unique zigzag edges.

## II. MODEL AND METHOD

When an O atom arbitrarily adsorbs on the wall of an intact SWNT, it will bond with two adjacent carbon atoms to form an epoxy group of C-O-C.<sup>21</sup> The underlying C-C bond is stretched by the interaction between O and C atoms. In each hexagonal carbon network, there are three possible orientations to form the epoxy group: one direction has a minimum angle  $\alpha$  to the nanotube longitudinal  $z$  axis, as show in Fig. 1, and the other two have an angle of  $\alpha+60^\circ$  and  $\alpha-60^\circ$  to the  $z$  axis, respectively. According to the definition of the nanotube chiral angle  $\theta$ , it can be easily deduced that  $\alpha=30^\circ-\theta$  and  $0^\circ\leq\alpha\leq30^\circ$ . For zigzag SWNTs, the  $\alpha=30^\circ$  direction is symmetrical with the  $\alpha-60^\circ$  direction while for armchair SWNTs,  $\alpha=0^\circ$ , and the  $\alpha+60^\circ$  direction is symmetrical with the  $\alpha-60^\circ$  direction. Furthermore, the C-O-C epoxy group can be defined as the unzipped epoxy or normal epoxy group depending on the underlying C-C bond

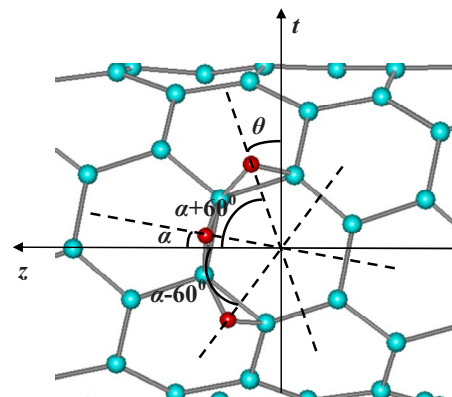


FIG. 1. (Color online) Three adsorption locations on a SWNT where O atom bonds with other two C atoms: one along the direction that has a minimum angle  $\alpha$  to the nanotube axis  $z$ , and other two direction  $\alpha+60^\circ$  and  $\alpha-60^\circ$  to the  $z$  axis.  $\theta$  with respect to the tangential direction  $t$  is the chiral angle of the nanotube. Here the red balls represent oxygen atoms and cyan balls represent carbon atoms.

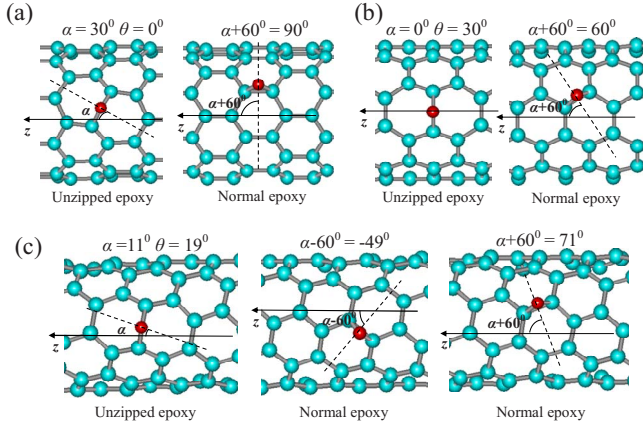


FIG. 2. (Color online) The formation of unzipped epoxy and normal epoxy groups when an O atom adsorbs on different sites of (a) (9, 0), (b) (5, 5), and (c) (6, 3) SWNTs.

broken or not broken.<sup>24</sup> As the curvature effect of the nanotube, the O adsorption on the three orientations will be different. It should be interesting to know whether one of the directions is energy optimum for O adsorption, and which kind of epoxy group will be formed.

We first investigate the adsorption of O atoms on SWNTs along the three possible directions. The computations were performed using the VASP code with the ultrasoft pseudopotential and local-density approximation for the exchange-correlation potential.<sup>25-27</sup> The periodic boundary with a large supercell in the longitudinal direction is applied for the SWNT. The length of the supercell and the separated distance between the adsorbed O atoms in the axially neighboring cells are chosen large enough to avoid any periodic interaction. An energy cutoff of 500 eV and special 16 *k* points uniformly sampled along the 1D Brillouin zone are used to ensure an energy convergence of less than 1 meV/atom. The whole system is fully relaxed using a conjugate-gradient algorithm until the force on each atom is less than 0.1 eV/nm.

III. RESULTS AND DISCUSSION

Figure 2 shows the optimized structures of an O atom adsorbing on different sites of (a) (9, 0), (b) (5, 5), and (c) (6, 3) SWNTs. The minimum angle  $\alpha$  to the tube axis for the three nanotubes is 30°, 0°, and 11°, respectively. There are only two adsorption directions for zigzag and armchair nanotubes because of structural symmetry. Different O-adsorption

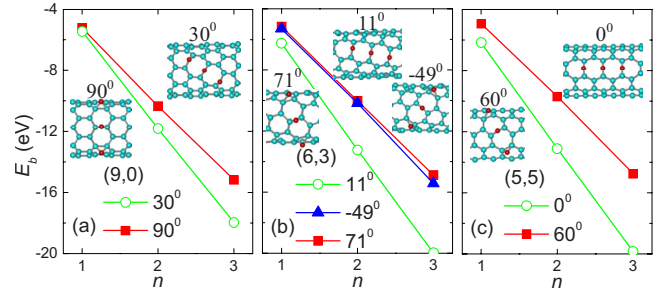


FIG. 3. (Color online) The binding energy  $E_b$  between O and SWNT versus the O atom number  $n$  for different adsorption directions. The insets show the optimized structures of three O atoms adsorbing on SWNTs.

site will lead to different kinds of epoxy group. For the (9,0) tube, the C-C distance beneath the O atom is 2.08 Å on the 30° adsorption direction and 1.46 Å on the 90° direction. The breaking of the C-C bond on the 30° direction means the formation of the unzipped epoxy group while the normal epoxy group is formed on the 90° direction. For the (5, 5) nanotube, the unzipped epoxy group is formed on the 0° direction, and the normal epoxy group is formed on the 60° direction, as shown in Fig. 2(b). Similarly, the unzipped epoxy group is formed on the direction of minimum angle to the (6, 3) tube axis, and on the other two directions are the normal epoxy groups [Fig. 2(c)].

Figure 3 shows the variations in binding energies with the number of O atoms adsorbing along different directions on (9, 0), (6, 3), and (5, 5) SWNTs after structural optimization. The binding energy is calculated by  $E_b = E_{CNT+O(n)} - E_{CNT} - E_{O(n)}$ , here  $E_{CNT+O(n)}$  is the total energy of the whole relaxed system,  $E_{CNT}$  and  $E_{O(n)}$  are the energies of free nanotube and free O atoms, and  $n$  is the number of O atoms. For one adsorbed O atom, the binding energy of the  $\alpha$  direction is slightly lower than that of other directions for all nanotubes as the formation of unzipped epoxy. When more O atoms adsorbing on the nanotubes, the binding energies of the  $\alpha$  direction are much lower than that of other direction. Thus, the direction that has a minimum angle to the tube axis is energetically favorable for O adsorption. The insets in Fig. 3 show the relaxed structures of three O atoms adsorbing along different directions. The C-C bonds beneath the O atoms are all broken (unzipped epoxy groups) for the case along the  $\alpha$  direction. For other directions, there are some underlying C-C bonds of epoxy groups broken with increasing the number of O atoms.

It has been previously reported that the most stable configuration for two O atoms adsorbing on graphene sheet is

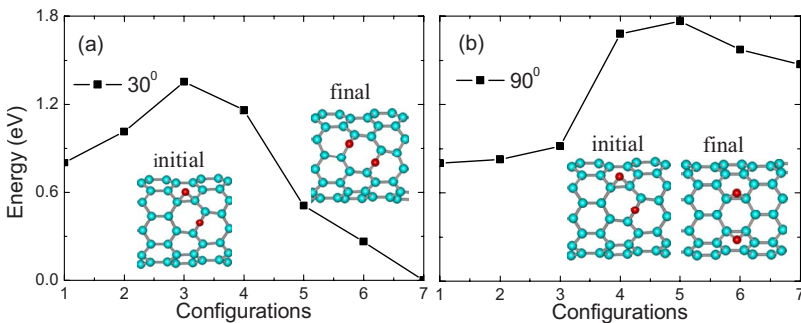


FIG. 4. (Color online) Minimum energy pathways of an O atom moving to the opposite end of an initial O atom adsorbing on the (9, 0) nanotube at the (a) 30° and (b) 90° directions. The insets show the initial and final configurations.

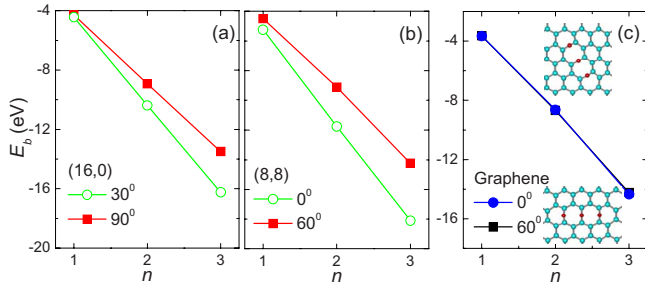


FIG. 5. (Color online) (a)–(c) The binding energy  $E_b$  of O adsorption on zigzag and armchair SWNTs of larger diameters, and flat graphene sheet. The insets show the optimized structures of three O atoms adsorbing along different directions.

that the two epoxy groups bind to the opposite ends of a hexagonal ring.<sup>21</sup> Using the density-functional theory (DFT)-based nudged elastic band method,<sup>28</sup> Fig. 4 shows the minimum energy paths for two O atoms adsorbing at the opposite sites on the (9, 0) nanotube but along different directions. The energy barrier for an O atom moving to the opposite end of an initial O atom adsorbing at the 30° direction is 0.55 eV while the energy barrier is 0.96 eV for O atoms at the 90° direction. As single O atom has no energy barrier to chemically adsorb onto a carbon nanotube, the diffusion energy barriers will determine the final distribution of O atoms on the tube. The lower energy barrier of the 30° direction confirms that O atom adsorbing along the  $\alpha$  direction of minimum angle to the nanotube axis is energetically favorable, and the subsequent O-adsorption locations will be in a line on the nanotube surface.

To probe the effect of nanotube diameter, we studied the energy-optimum O adsorption on larger diameter SWNTs. Similarly, for both (16, 0) and (8, 8) nanotubes the binding energies of the O adsorption along the direction of minimum angle to the axis is lower than other directions [Figs. 5(a) and 5(b)]. Along the energy optimum directions, the formed epoxy groups are all the unzipped epoxy. Furthermore, the

energy-optimum O-adsorption sites are consistent with previous theoretical predications.<sup>29,30</sup> The nanotube curvature leads to larger local deformation of the C-C bonds on the energy-optimum direction and stronger changing in the  $sp^2$  hybridization of the C-C bonds.<sup>29,30</sup> This makes those C-C bonds possess higher chemical activity to bond with O atoms. Nevertheless, comparing with (9, 0) and (5, 5) nanotubes the energy difference between the optimum direction and other directions decreases with increasing nanotube diameters. The curvature effect on the C-C bonds disappears when the nanotube becomes a flat graphene sheet. Accordingly there is no any curvature effect on the O-adsorption direction. As shown in Fig. 5(c), the binding energies of O adsorption on flat graphene sheet are approximately the same for two adsorption directions. This indicates that the energy-optimum O adsorption depends on the nanotube diameter.

The normal epoxy groups will become the unzipped epoxy groups when more and more O atoms adsorb on the same direction (opposite end) of the nanotubes because those O atoms can provide enough strain energy to break the underlying C-C bonds.<sup>21</sup> Thus, long unzipped epoxy chains may form on the nanotubes for the three O-adsorption directions shown in Fig. 1. As limited by the calculation ability of the DFT technique, we establish a simple elastic theory model to investigate which direction on the SWNT is energetically favorable for the formation of long unzipped epoxy chains. Here we assume that the interaction for breaking the normal epoxy into unzipped epoxy is caused by the force between O and C atoms. Then the force to break the C-C bond can be decomposed into a stretching force  $F_s$  along the C-C bond, and another  $F_r$  along the radial direction [Fig. 6(a)]. The stretching force  $F_s$  plays a dominating role in the interaction between O and C atoms. On the other hand, the stretching force  $F_s$  on the C-C bond can also be decomposed into two components:  $F_z$  along the axis of the nanotube, and  $F_t$  along the tangential direction of the circumference of the nanotube, as shown in Figs. 6(b) and 6(c). The strain energy induced by the axial force  $F_z$  can be approximately expressed as

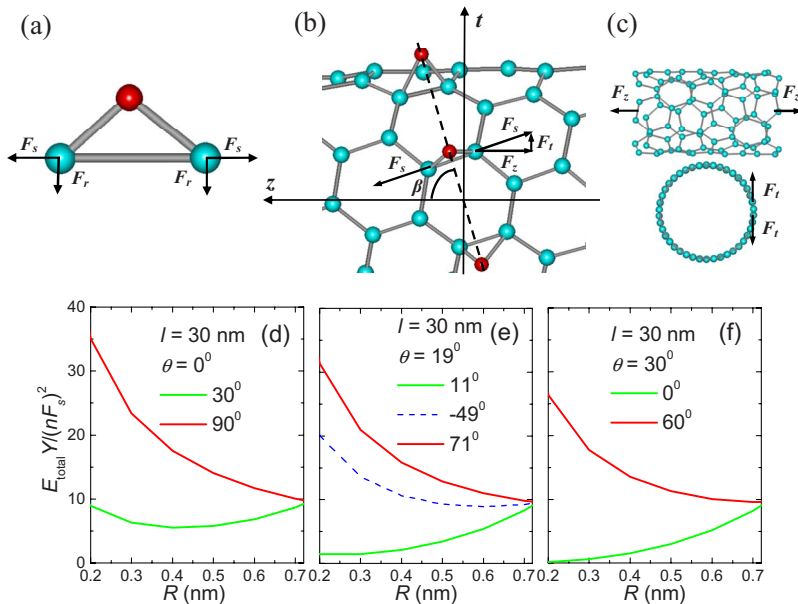


FIG. 6. (Color online) (a) The geometry of the force acting on the C-C bond in a normal epoxy group, which imposed by one O atom. (b) The stretching force  $F_s$  is decomposed into two forces  $F_z$  and  $F_t$ . Here the red atoms are oxygen and cyan atoms are carbon. (c) Display of the effects of the longitudinal force  $F_z$  and the tangential force  $F_t$  on SWNT. (d)–(f) The variations in  $E_{total} Y / (n F_s)^2$  with  $R$  for different direction  $\beta$ , and the nanotubes have chiral angle  $\theta=0^\circ, 19^\circ$ , and  $30^\circ$ .

$$E_z = \frac{F_z^2 l}{2YA} = \frac{F_z^2 l}{4\pi YRh} \quad (1)$$

and the strain energy induced by the tangential force approximately is

$$E_t = \frac{1}{2} F_t \frac{3\pi R^3 F_t}{2YI} = \frac{9\pi R^3 F_t^2}{Yh^3 l}. \quad (2)$$

Here  $Y$  is Young's modulus;  $R$  is the nanotube radius,  $l$  is the nanotube length, and  $h$  is the thickness of the nanotube. We assume that the elastic modulus  $Y$  of the nanotube is the same for both of axial and tangential directions and the thickness  $h$  is taken as 0.34 nm.<sup>31–33</sup> According to the geometry shown in Figs. 6(a) and 6(b), the total unzipping strain energy  $E_{total}$  induced by an epoxy chain on SWNT is

$$\begin{aligned} E_{total} &= E_t + E_z = \frac{9\pi R^3 (nF_t)^2}{Yh^3 l} + \frac{(nF_z)^2 l}{4\pi YhR} \\ &= \frac{9\pi R^3 [nF_s \sin(90^\circ - \beta)]^2}{Yh^3 l} + \frac{[nF_s \cos(90^\circ - \beta)]^2 l}{4\pi YhR}. \end{aligned} \quad (3)$$

Here  $n$  is the number of O atoms and  $\beta$  is the angle of epoxy chain formation direction to the  $z$  axis [Fig. 6(b)], which is also equivalent to the O-adsorption direction shown in Fig. 1 and could be  $\alpha$ ,  $\alpha - 60^\circ$ , or  $\alpha + 60^\circ$ .

We assume that each O atom imposes the same stretching force  $F_s$  on each C atom of the normal epoxy groups, and the force  $F_s$  can be considered as approximate constant but its value cannot be directly deduced out. However, the  $E_{total} Y / (nF_s)^2$  can be calculated out by the  $\beta$ ,  $R$ ,  $l$ , and  $h$  in term of the Eq. (3). The magnitude of  $E_{total} Y / (nF_s)^2$  just represents the magnitude of strain energy  $E_{total}$  needed to break the normal epoxy into unzipped epoxy, as the  $F_s$ ,  $Y$ , and  $n$  are constant. Figures 6(d)–6(f) show the variations in  $E_{total} Y / (nF_s)^2$  with tube radius  $R$  for different formation directions of unzipped epoxy chains on zigzag, chiral, and armchair SWNTs. Low  $E_{total} Y / (nF_s)^2$  means low strain energy that is needed for O atoms to break the underlying C-C bonds, and the normal epoxy groups are more favorable to transform into unzipped epoxy groups. Obviously, over a large size range up to  $R=0.7$  nm, the strain energies remain to be the lowest for the unzipped epoxy chains formed along the direction of minimum angle to the  $z$  axis. These energy-optimum directions for unzipped epoxy chains are exactly coincident with the energy-optimum directions to form the unzipped C-O-C groups predicted by the DFT calculations as shown in Figs. 2 and 3. Therefore, the energy-optimum direction for O adsorption on the nanotube and that for the formation of the unzipped epoxy chain are the same. This will lead to unique unzipping direction of the nanotube. However, the strain energy difference between different directions decreases with increasing  $R$ . For long nanotubes with length of about 30 nm, the energy differences will die out when tube radius is larger than about 0.7 nm, indicating that the nanotubes with diameter larger than 1.4 nm will loss such energy favorability. As a consequence, under experi-

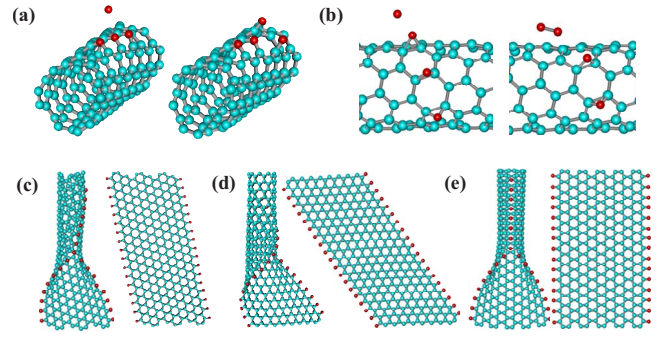


FIG. 7. (Color online) Initial and final optimized structures of a free O atom attacking (a) an unzipped epoxy group forming on the energetically optimum O-adsorption sites (along the  $11^\circ$  direction) of the (6, 3) SWNT, and (b) a normal epoxy group on other O-adsorption sites (along the  $71^\circ$  direction) of the (6, 3) nanotube. (c)–(e) Predicted displays of oxidatively opening (6, 3), (9, 0), and (5, 5) SWNTs into zigzag graphene nanoribbons along the energy-optimum directions.

mental conditions small-diameter SWNTs are prone to be oxidized and unzipped along the energy-optimum direction.

The unzipped epoxy sites on a SWNT are still chemical active parts, which can easily interact with other O atoms.<sup>22</sup> We consider that a (6, 3) nanotube on which unzipped epoxy groups have been formed along the energy-optimum direction is attacked by a free O atom, and the whole structure is then relaxed by using the same DFT technique [Fig. 7(a)]. After optimization, one of epoxy groups is broken into two carbonyl groups, and the nanotube is broken at this defect. This is consistent with oxidative cut of graphene by forming unzipped epoxy and then carbonyl pairs.<sup>23</sup> Moreover, we have also investigated whether the free O atom could break the normal epoxy group formed on the other direction of the (6, 3) nanotube. It is shown from Fig. 7(b) that the O atom in the normal epoxy group is dragged out and forms oxygen molecular with the free O atom without any change on the nanotube. According to our DFT calculations, the binding energies of an oxygen molecule and a C-O bond are 7.42 eV and 5.5 eV, respectively. From the energetics viewpoint, the formation of the carbonyl pair (two C-O bonds formed) when a free O atom attacks the unzipped epoxy group is therefore energetically favorable. While the C-C bond of the normal epoxy group is slightly stretched, and the binding energy of a C-C bond is 10.9 eV. If the normal epoxy group is broken into carbonyl pair by a free O atom, it will have to break the underlying C-C bond and a C-O bond. However, this process is not energetically favorable after carefully comparing the binding energies of C-C, C-O, and O-O bonds. As a consequence, the free O atom is favorable to bond with the O atom rather than the C atoms in the normal epoxy group.

According to these DFT results and the above theoretical model, it can be expected that the (6, 3) SWNT should be opened along the energy-optimum direction with more O atoms interacting with the unzipped epoxy chain, and will transform into a graphene nanoribbon of zigzag edges and small width, as shown in Fig. 7(c). Other zigzag and armchair SWNTs could be opened into graphene nanoribbons

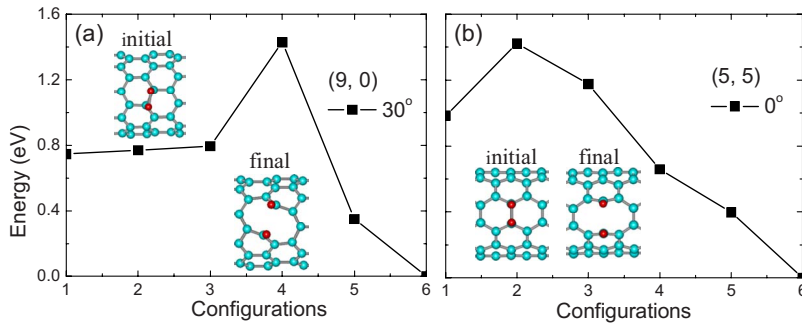


FIG. 8. (Color online) The energy barrier for an oxygen molecule transforming into carbonyl pair, which adsorbs (a) at the  $30^\circ$  direction of the (9, 0) nanotube and (b) at the  $0^\circ$  direction of the (5, 5) nanotube. The insets show the initial and final configurations.

applying the same oxidative process [Figs. 7(d) and 7(e)]. The edges of the obtained nanoribbons are unique zigzag, and the widths of the unzipped nanoribbon along the energy-optimum direction are the smallest comparing with other unzipping directions and equal to  $w=2\pi R \sin(\theta+60^\circ)$ . Except armchair nanotubes opened along the axial direction, other chiral nanotubes will be opened along a spiral line around the nanotubes.

We have also studied the effect of adsorption of an oxygen molecule on the structure of SWNT. When an oxygen molecule adsorb on the  $30^\circ$  direction of the (9, 0) nanotube, the length of the underlying C-C bond is stretched to 1.57 Å and this C-C bond is not broken, as shown by the initial state of the insets in Fig. 8(a). For an oxygen molecule adsorbing on the  $0^\circ$  direction of the (5, 5) nanotube, the underlying C-C bond is stretched to 1.62 Å and not broken as well [Fig. 8(b)]. The oxygen molecule cannot unzip the C-C bond as the oxygen atom adsorbing on the energy-optimum direction. This is because that the chemical activity of an oxygen molecule is lower than that of a free O atom and it cannot afford enough energy to break the C-C bond. Our DFT calculations show that the unzipped epoxy group is energetically preferable to be broken into carbonyl pair when it interacts with a free O atom. To compare with the transition process of the unzipped epoxy group, we use the DFT-based nudged elastic band method<sup>28</sup> to calculate the energetic changes for the transformation of the adsorbed oxygen molecules on the (9, 0) and (5, 5) nanotubes into carbonyl pairs, as shown in Fig. 8. For both (9, 0) and (5, 5) nanotubes, the energies of car-

bonyl pair states are lower than that of the adsorption states. However, the energy barriers for the oxygen molecule to carbonyl pair on the (9, 0) and (5, 5) nanotubes are 0.68 eV and 0.44 eV, respectively. Different from O atom, the adsorption of an oxygen molecule will not lead to the unzipping of the nanotube.

#### IV. CONCLUSION

In summary, DFT calculations demonstrate that on small-diameter SWNTs O atoms are prone to adsorb and form unzipped epoxy groups along an energetically favorable direction, which has a minimum angle to the nanotube axial direction. Theoretical model analysis reveals the same energy-optimum direction for the formation of unzipped epoxy chains on the SWNTs of small diameters. Carbon nanotubes could be opened into graphene nanoribbons of all zigzag edges and minimum widths by oxidizing the existed unzipped epoxy chains formed on the energy-optimum direction. Our study unveils some fundamental oxidation behaviors on carbon nanotubes, and presents an insight into controllable fabrication of graphene nanoribbons.

#### ACKNOWLEDGMENTS

This work is supported by the 973 Program (Grant No. 2007CB936204), NSF (Grants No. 10732040, No. 10947156, and No. 11072109), Jiangsu NSF (BK2009365) of China, and Innovation Fund of NUA.

\*yfguo@nuaa.edu.cn

†wlguo@nuaa.edu.cn

<sup>1</sup>K. Novoselov, *Nature Mater.* **6**, 720 (2007).

<sup>2</sup>M. Y. Han, B. Ozyilmaz, Y. Zhang, and P. Kim, *Phys. Rev. Lett.* **98**, 206805 (2007).

<sup>3</sup>H. Qian, F. Negri, C. Wang, and Z. Wang, *J. Am. Chem. Soc.* **130**, 17970 (2008).

<sup>4</sup>L. Yang, C. H. Park, Y. W. Son, M. L. Cohen, and S. G. Louie, *Phys. Rev. Lett.* **99**, 186801 (2007).

<sup>5</sup>O. Hod, V. Barone, J. E. Peralta, and G. E. Scuseria, *Nano Lett.* **7**, 2295 (2007).

<sup>6</sup>K. Nakada, M. Fujita, G. Dresselhaus, and M. S. Dresselhaus, *Phys. Rev. B* **54**, 17954 (1996).

<sup>7</sup>Y. W. Son, M. L. Cohen, and S. G. Louie, *Nature (London)* **444**,

347 (2006).

<sup>8</sup>X. Wang, Y. Ouyang, X. Li, H. Wang, J. Guo, and H. J. Dai, *Phys. Rev. Lett.* **100**, 206803 (2008).

<sup>9</sup>S. Dutta, A. K. Manna, and S. K. Pati, *Phys. Rev. Lett.* **102**, 096601 (2009).

<sup>10</sup>Y. F. Guo, W. L. Guo, and C. F. Chen, *J. Phys. Chem. C* **114**, 13098 (2010).

<sup>11</sup>Z. H. Zhang, C. F. Chen, and W. L. Guo, *Phys. Rev. Lett.* **103**, 187204 (2009).

<sup>12</sup>D. V. Kosynkin, A. L. Higginbotham, A. Sinitskii, J. R. Lomeda, A. Dimiev, B. K. Price, and J. M. Tour, *Nature (London)* **458**, 872 (2009).

<sup>13</sup>A. G. Cano-Márquez, F. J. Rodríguez-Macías, J. Campos-Delgado, C. G. Espinosa-González, F. Tristán-López, D.

- Ramírez-González, D. A. Cullen, D. J. Smith, M. Terrones, and Y. I. Vega-Cantú, *Nano Lett.* **9**, 1527 (2009).
- <sup>14</sup>L. Y. Jiao, L. Zhang, X. R. Wang, G. Diankov, and H. J. Dai, *Nature (London)* **458**, 877 (2009).
- <sup>15</sup>F. Cataldo, G. Compagnini, G. Patané, O. Ursini, G. Angelini, P. R. Ribic, G. Margaritondo, A. Cricenti, G. Palleschi, and F. Valentini, *Carbon* **48**, 2596 (2010).
- <sup>16</sup>P. M. Ajayan and S. Iijima, *Nature (London)* **361**, 333 (1993).
- <sup>17</sup>J. Liu, A. G. Rinzler, H. Dai, J. H. Hafner, R. K. Bradley, P. J. Boul, A. Lu, T. Iverson, K. Shelimov, C. B. Huffman, F. Rodriguez-Macias, Y.-S. Shon, T. R. Lee, D. T. Colbert, and R. E. Smalley, *Science* **280**, 1253 (1998).
- <sup>18</sup>S. S. Alexandre, M. S. C. Mazzoni, and H. Chacham, *Phys. Rev. Lett.* **100**, 146801 (2008).
- <sup>19</sup>J. A. Yan, L. D. Xian, and M. Y. Chou, *Phys. Rev. Lett.* **103**, 086802 (2009).
- <sup>20</sup>M. K. Ashraf, N. A. Bruque, R. R. Pandey, P. G. Collins, and R. K. Lake, *Phys. Rev. B* **79**, 115428 (2009).
- <sup>21</sup>J. L. Li, K. N. Kudin, M. J. McAllister, R. K. Prud'homme, I. A. Aksay, and R. Car, *Phys. Rev. Lett.* **96**, 176101 (2006).
- <sup>22</sup>N. L. Rangel, J. C. Sotelo, and J. M. Seminario, *J. Chem. Phys.* **131**, 031105 (2009).
- <sup>23</sup>Z. Li, W. Zhang, Y. Luo, J. Yang, and J. G. Hou, *J. Am. Chem. Soc.* **131**, 6320 (2009).
- <sup>24</sup>H. Xiang, S. Wei, and X. Gong, [arXiv:1001.0171](https://arxiv.org/abs/1001.0171) (unpublished).
- <sup>25</sup>G. Kresse and J. Hafner, *Phys. Rev. B* **47**, 558 (1993).
- <sup>26</sup>G. Kresse and J. Hafner, *Phys. Rev. B* **49**, 14251 (1994).
- <sup>27</sup>D. Vanderbilt, *Phys. Rev. B* **41**, 7892 (1990).
- <sup>28</sup>G. Mills, H. Jonsson, and G. K. Schenter, *Surf. Sci.* **324**, 305 (1995).
- <sup>29</sup>G. E. Froudakis, M. Schnell, M. Mühlhäuser, S. D. Peyerimhoff, A. N. Andriotis, M. Menon, and R. M. Sheetz, *Phys. Rev. B* **68**, 115435 (2003).
- <sup>30</sup>H. J. Liu, C. T. Chan, Z. Y. Liu, and J. Shi, *Phys. Rev. B* **72**, 075437 (2005).
- <sup>31</sup>J. P. Lu, *Phys. Rev. Lett.* **79**, 1297 (1997).
- <sup>32</sup>E. Hernández, C. Goze, P. Bernier, and A. Rubio, *Phys. Rev. Lett.* **80**, 4502 (1998).
- <sup>33</sup>C. Li and T. W. Chou, *Int. J. Solids Struct.* **40**, 2487 (2003).